A joint atmosphere-ocean inversion for surface fluxes of carbon dioxide: 2. Regional results

Andrew R. Jacobson,[1,2] Sara E. Mikaloff Fletcher,[1,3] Nicolas Gruber,[3,4] Jorge L. Sarmiento,[1] and Manuel Gloor[1,5]

Received 31 January 2006; revised 4 November 2006; accepted 27 November 2006; published 17 March 2007.

[1] We report here the results from a coupled ocean-atmosphere inversion, in which atmospheric CO_2 gradients and transport simulations are combined with observations of ocean interior carbon concentrations and ocean transport simulations to provide a jointly constrained estimate of air-sea and air-land carbon fluxes. While atmospheric data have little impact on regional air-sea flux estimates, the inclusion of ocean data drives a substantial change in terrestrial flux estimates. Our results indicate that the tropical and southern land regions together are a large source of carbon, with a 77% probability that their aggregate source size exceeds 1 PgC yr^{-1}. This value is of similar magnitude to estimates of fluxes in the tropics due to land-use change alone, making the existence of a large tropical CO_2 fertilization sink unlikely. This terrestrial result is strongly driven by oceanic inversion results that differ from flux estimates based on ΔpCO_2 climatologies, including a relatively small Southern Ocean sink (south of 44°S) and a relatively large sink in the southern temperate latitudes (44°S–18°S). These conclusions are based on a formal error analysis of the results, which includes uncertainties due to observational error transport and other modeling errors, and biogeochemical assumptions. A suite of sensitivity tests shows that these results are generally robust, but they remain subject to potential sources of unquantified error stemming from the use of large inversion regions and transport biases common to the suite of available transport models.

Citation: Jacobson, A. R., S. E. Mikaloff Fletcher, N. Gruber, J. L. Sarmiento, and M. Gloor (2007), A joint atmosphere-ocean inversion for surface fluxes of carbon dioxide: 2. Regional results, *Global Biogeochem. Cycles*, *21*, GB1020, doi:10.1029/2006GB002703.

1. Introduction

[2] This manuscript is concerned with interpretation of flux estimates from a joint ocean-atmosphere inversion introduced in a companion paper [*Jacobson et al.*, 2007]. This joint inversion combines atmospheric and oceanic carbon observations with multiple transport simulations (16 in the atmosphere and 10 in the ocean) to produce estimates of surface fluxes. Results are produced independently for each unique combination of atmospheric and oceanic transport simulation, and the resulting ensemble of 160 permutations thus includes a sample of uncertainty due to errors in transport modeling. Details of the construction of this joint inverse, discussion of its limitations, and results on global scales are presented by *Jacobson et al.* [2007].

[3] As described by *Jacobson et al.* [2007], the joint inversion does not use regularization techniques to decrease flux uncertainties. It thus admits larger uncertainties for underobserved land regions than inversions that use model-based priors to blend observationally derived fluxes with predictions from terrestrial carbon simulations. In the atmospheric inversion, a sparse observational data set combined with diffusive transport results in regions whose fluxes cannot be effectively distinguished from one another. The present unregularized atmospheric inversion preserves the raw correlations between such flux regions. It is via these correlations that information from the ocean interior is transmitted to terrestrial flux estimates in the joint inversion. Contemporary air-sea fluxes from the present oceanic inversion differ significantly from forward simulations and estimates based on ΔpCO_2 observations. These differences drive a reinterpretation of terrestrial fluxes in the tropics and Southern Hemisphere, suggesting that these regions may be

[1]Atmospheric and Oceanic Sciences Program, Princeton University, Princeton, New Jersey, USA.
[2]Earth System Research Laboratory, NOAA, Boulder, Colorado, USA.
[3]Department of Atmospheric and Oceanic Sciences, University of California, Los Angeles, California, USA.
[4]Institute of Biogeochemistry and Pollutant Dynamics, ETH Zurich, Zurich, Switzerland.
[5]Earth and Biosphere Institute and School of Geography, University of Leeds, Leeds, UK.

0886-6236/07/2006GB002703$12.00

Table 1. Comparison of Various Contemporary (Anthropogenic ± Preindustrial) CO_2 Surface Flux Estimates Using the Inversion Convention of Attributing the Outgassing of River Carbon Entirely to the Ocean[a]

Region Number	Full Name	Abbrev.	Tak99	Tak02	T3L1	T3L2	MOM3 Forward	Atmospheric	Joint
1	North American Boreal	NABR			0.26 ± 0.48	0.20 ± 0.33		0.50 ± 0.92	−0.13 ± 0.64
2	North American Temperate	NATM			−0.81 ± 0.72	**−0.89 ± 0.39**		−1.06 ± 1.07	−0.93 ± 0.76
3	South American Tropical	SATR			0.63 ± 1.21	0.74 ± 1.06		4.69 ± 5.88	**3.07 ± 2.36**
4	South American Temperate	SATM			−0.16 ± 1.01	−0.24 ± 0.88		−2.80 ± 4.67	−0.84 ± 1.72
5	Northern Africa	NAFR			−0.17 ± 1.28	0.79 ± 1.01		3.58 ± 5.37	1.62 ± 2.95
6	Southern Africa	SAFR			−0.32 ± 1.02	−0.51 ± 0.84		−0.69 ± 5.41	−1.74 ± 2.57
7	Eurasia Boreal	EUBR			−0.52 ± 0.76	−0.36 ± 0.56		−0.60 ± 1.01	0.04 ± 0.72
8	Eurasia Temperate	EUTM			−0.63 ± 0.89	−0.41 ± 0.81		−0.21 ± 1.79	−0.81 ± 1.20
9	Tropical Asia	ASTR			0.68 ± 0.87	0.27 ± 1.04		−2.60 ± 4.95	−0.50 ± 2.19
10	Australia	AUST			0.32 ± 0.35	−0.10 ± 0.22		−0.18 ± 0.57	0.15 ± 0.35
11	Europe	EURO			−0.61 ± 0.57	**−0.96 ± 0.47**		−0.63 ± 0.79	**−1.05 ± 0.54**
12	North Pacific Temperate	NPTM	−0.39	−0.41	−0.27 ± 0.46	−0.31 ± 0.31	**−0.54 ± 0.04**	−0.16 ± 0.62	**−0.45 ± 0.08**
13	West Pacific Tropical	WPTR	0.16	0.16	−0.16 ± 0.40	−0.21 ± 0.32	**0.03 ± 0.02**	−0.21 ± 1.01	**0.12 ± 0.07**
14	East Pacific Tropical	EPTR	0.47	0.52	**0.64 ± 0.42**	0.66 ± **0.33**	0.42 ± **0.04**	0.24 ± 1.66	**0.31 ± 0.03**
15	South Pacific Temperate	SPTM	−0.21	−0.28	0.06 ± 0.68	0.51 ± 0.57	**−0.30 ± 0.04**	0.52 ± 1.18	**−0.50 ± 0.07**
16	Northern Ocean	NOCN	−0.41	−0.24	**−0.33 ± 0.24**	−0.28 ± **0.19**	−0.30 ± **0.01**	−0.47 ± 0.41	**−0.21 ± 0.07**
17	North Atlantic Temperate	NATM	−0.21	−0.22	−0.42 ± 0.43	−0.29 ± 0.33	**−0.29 ± 0.02**	−1.01 ± 1.35	**−0.40 ± 0.06**
18	Atlantic Tropical	SATR	0.24	0.25	−0.03 ± 0.35	−0.10 ± 0.24	**0.24 ± 0.01**	−1.51 ± 2.15	**0.20 ± 0.11**
19	South Atlantic Temperate	SATM	−0.07	−0.15	0.02 ± 0.43	−0.05 ± 0.25	**−0.09 ± 0.01**	1.30 ± 2.41	**−0.24 ± 0.05**
20	Southern Ocean	SOCN	−0.99	−0.58	**−0.58 ± 0.37**	−0.55 ± **0.37**	−0.59 ± **0.14**	−0.63 ± 0.60	**−0.15 ± 0.07**
21	Indian Tropical	INTR	0.18	0.24	−0.10 ± 0.48	−0.32 ± 0.33	**0.06 ± 0.01**	−0.39 ± 1.03	**0.13 ± 0.07**
22	Indian Temperate	INTM	−0.48	−0.47	−0.26 ± 0.39	**−0.39 ± 0.29**	−0.37 ± **0.03**	−0.52 ± 0.74	**−0.52 ± 0.04**
1,2,7,8,11	Northern Land				**−2.31 ± 1.06**	−2.42 ± **1.13**		−2.00 ± 2.14	**−2.89 ± 1.05**
12,16,17	Northern Ocean		−1.00	−0.86	−1.03 ± 0.81	**−0.88 ± 0.56**	−1.13 ± **0.07**	−1.64 ± 1.78	**−1.06 ± 0.12**
3,5,9	Tropical Land				1.13 ± 1.75	1.80 ± 1.83		5.68 ± 7.10	**4.20 ± 2.72**
13,14,18,21	Tropical Ocean		1.05	1.17	0.34 ± 0.81	0.03 ± 0.55	**0.76 ± 0.09**	−1.87 ± 2.70	**0.76 ± 0.14**
4,6,10	Southern Land				−0.16 ± 1.29	−0.85 ± 1.17		−3.67 ± 5.89	−2.43 ± 2.02
15,19,20,22	Ocean in South		−1.74	−1.48	−0.77 ± 0.80	−0.49 ± 0.64	**−1.35 ± 0.23**	0.68 ± 2.21	**−1.40 ± 0.10**
12,15,17,19,22	Temperate Oceans		−1.35	−1.53	−0.88 ± 1.06	−0.54 ± 0.83	**−1.59 ± 0.14**	0.14 ± 2.65	**−2.11 ± 0.15**
16,20	High−Latitude Oceans		−1.40	−0.81	**−0.91 ± 0.50**	**−0.83 ± 0.38**	**−0.89 ± 0.16**	**−1.09 ± 0.81**	**−0.35 ± 0.08**
3−6,9,10	Tropical and Southern Land				0.97 ± 1.47	0.95 ± 1.40		2.00 ± 4.10	**1.77 ± 1.06**
1−11	All Land				−1.34 ± 1.38	**−1.47 ± 0.98**		0.00 ± 3.25	**−1.12 ± 0.23**
12−22	All Ocean		−1.70	−1.18	−1.45 ± 1.38	**−1.34 ± 0.98**	**−1.72 ± 0.38**	−2.83 ± 3.25	**−1.71 ± 0.22**
1−22	Global				**−2.78 ± 0.07**	**−2.80 ± 0.01**		**−2.83 ± 0.07**	**−2.83 ± 0.07**

[a]See auxiliary material of *Jacobson et al.* [2007]. A positive flux represents input to the atmosphere. Results are presented for the 22 regions of the TransCom3 protocol [*Gurney et al.*, 2002] and 12 aggregates as the annual over the period 1992–1996. The estimates are Tak99 [*Takahashi et al.*, 1999], Tak02 [*Takahashi et al.*, 2002], T3L1 [*Gurney et al.*, 2002] T3L2 [*Gurney et al.*, 2004], MOM3 Forward (forward simulations of MOM3 suite using OCMIP2 biotic protocol), Atmospheric (current unregularized atmospheric inversion), and joint (current joint inversion). Uncertainties are presented as 1 standard deviation and include within- and across-model variance (MOM3 forward simulations have no within-model uncertainty estimates). Estimates that are significantly different from zero at the 90% confidence level (one-sided probability using marginal densities) are shown in bold.

a large and statistically significant source of CO_2 to the atmosphere, a result not formally detected in previous atmospheric inversions [*Heimann*, 2001; *Gurney et al.*, 2002; *Rödenbeck et al.*, 2003b; *Gurney et al.*, 2004].

2. Results and Discussion

[4] Estimates of surface fluxes of carbon dioxide over the 1992–1996 period are presented for 11 ocean and 11 land regions in Table 1. These are compared to various other flux estimates, including the ΔpCO_2-based estimates of *Takahashi et al.* [1999, 2002], forward simulations of ocean carbon models, and atmospheric inversions from the TransCom3 project ("T3L1" [*Gurney et al.* 2002] and "T3L2" [*Gurney et al.* 2004]).

[5] In what follows, we discuss first the air-sea flux estimates from the joint inversion, then the terrestrial flux estimates. The joint inversion suggests that the land regions of the tropics and Southern Hemisphere comprise a remarkable source of carbon, and the remainder of the paper is concerned with evaluating the reliability of this result. This includes an exploration of reasons why such a source could have gone undetected in previous inversions, a set of sensitivity tests, and a discussion of the oceanographic reasons for this result.

2.1. Ocean Fluxes in Detail

[6] The ocean inversion estimates a global preindustrial air-sea flux source $\Phi_{\text{preindust}}$ of 0.39 ± 0.05 PgC yr^{-1} and an anthropogenic global flux Φ_{anthro} of −2.1 ± 0.1 PgC yr^{-1} for the 1992–1996 period (Table 1). The anthropogenic global flux estimate is in line with predictions from forward simulations and pCO_2-based methods, analyses of atmospheric oxygen and ^{13}C concentrations [*Le Quéré et al.*, 2003], and other ocean inversions [*Gloor et al.*, 2003; *Mikaloff Fletcher et al.*, 2006]. As discussed in the auxiliary material of *Jacobson et al.* [2007], $\Phi_{\text{preindust}}$ includes a correction of 0.45 PgC yr^{-1} for river carbon delivered to the open ocean. Ocean inversions, ΔpCO_2-based flux estimates, and forward simulations agree that tropical ocean

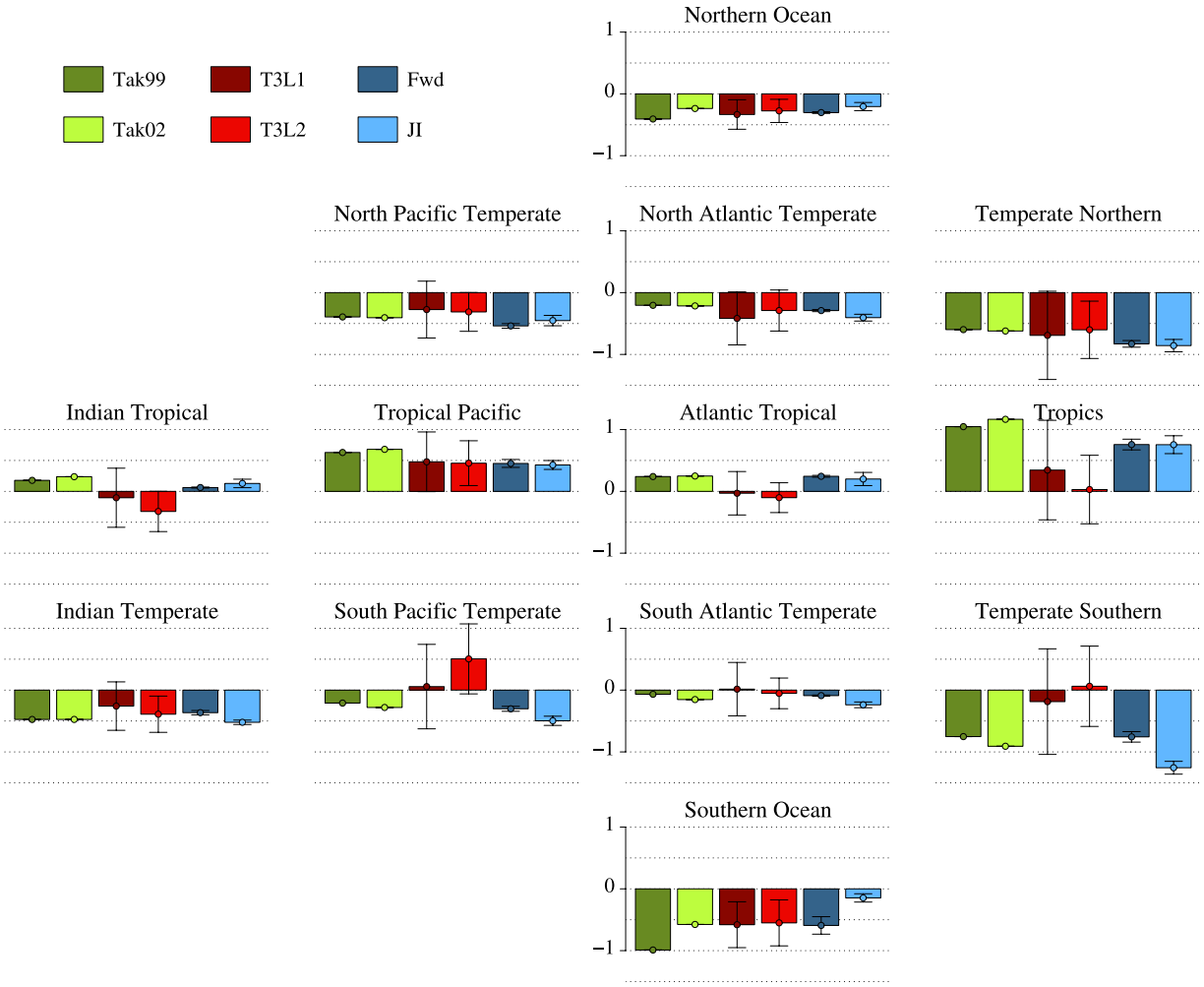

Figure 1. Contemporary air-sea flux estimates (anthropogenic + preindustrial in PgC yr^{-1}) arranged in approximate geographic location from various sources. The first three columns of this tableau correspond to the Indian Ocean, the Pacific Ocean, and the Atlantic Ocean, respectively. The fourth column portrays estimates aggregated across basins by latitude band. The estimates are Tak99 [*Takahashi et al.*, 1999], Tak02 [*Takahashi et al.*, 2002], T3L1 [*Gurney et al.*, 2002], T3L2 [*Gurney et al.*, 2004], Fwd (forward simulations of MOM3 suite using the Ocean Carbon Model Intercomparison Project 2 [*Orr et al.*, 2001] biotic protocol), and JI (current joint inversion). Error bars represent 1 standard deviation for estimates that include uncertainties. The ΔpCO_2-based estimates are all referenced to 1995; all others are the mean over 1992–1996.

regions are sources of CO_2 to the atmosphere, with the greatest contribution coming from the Pacific ocean (Figure 1 and Table 1). While the differences individually are not statistically significant owing to the estimated uncertainties of the inversion results, each forward simulation predicts about 0.1 PgC yr^{-1} more anthropogenic uptake than inverse models.

[7] We turn now to comparing regional estimates of contemporary air-sea fluxes from our joint inversion with those of other methods. These contemporary fluxes represent the sum of the preindustrial and anthropogenic air-sea fluxes, $\Phi_{contemp} = \Phi_{preindust} + \Phi_{anthro}$, and are referenced to the 1992–1996 annual mean. Contemporary fluxes are used since the methods with which we will be comparing do not distinguish preindustrial from anthropogenic fluxes. These fluxes are summarized in Table 1 and Figure 1.

[8] Our joint inversion suggests a smaller contemporary outgassing in the eastern equatorial Pacific than the pCO_2-based flux estimates of *Takahashi et al.* [2002] (henceforth, Tak02). There are significant uncertainties in the pCO_2 estimates stemming from temporal and spatial extrapolation of sparse observations [*Fung and Takahashi*, 2000], and flux estimates made from the resultant pCO_2 estimates are subject to further sources of error as uncertain wind speed estimates are combined with uncertain bulk gas transfer parameterizations [*Wanninkhof and McGillis*, 1999; *Feely et al.*, 2001, 2004]. A potential explanation for the difference seen here is that the Tak02 product specifically excludes

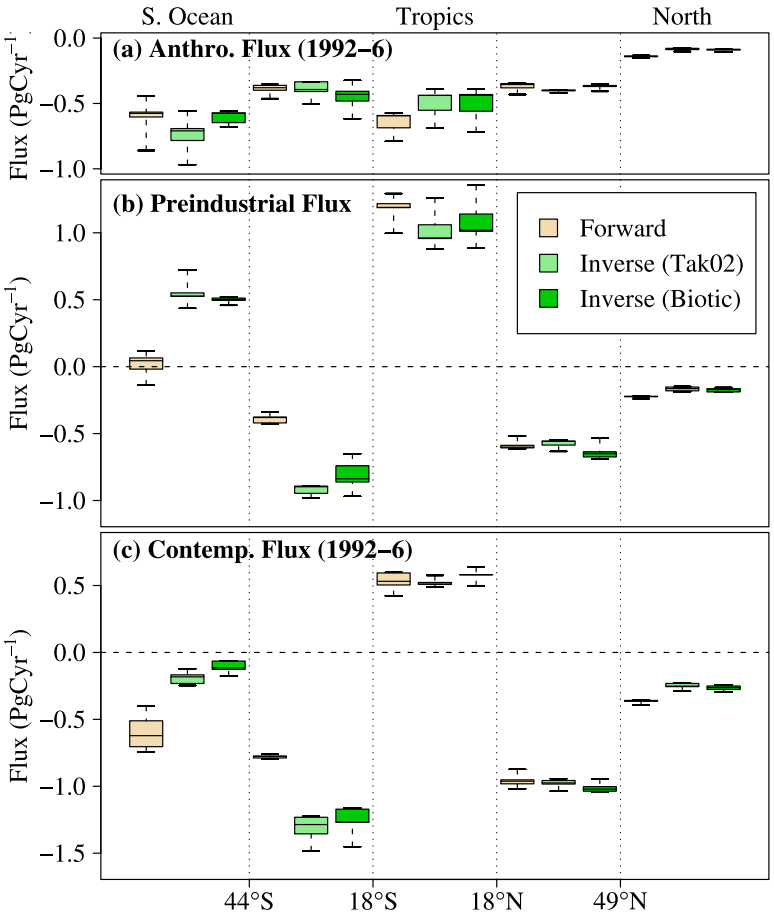

Figure 2. Zonally integrated air-sea flux estimates from ocean inversions and forward simulations for (a) anthropogenic flux, (b) preindustrial flux, and (c) contemporary flux. Within each latitude band, forward simulations of the MOM3 suite using the OCMIP2 biotic protocol [*Orr et al.*, 2001] ("Forward") are shown in tan, and inverse estimates are given for two different within-region flux patterns ("Tak02," light green: *Takahashi et al.* [2002] flux patterns; "Biotic," dark green: flux patterns determined from forward simulations), from left to right, respectively. The colored boxes have boundaries at the 25th and 75th percentiles, and the interior line is at the median. Error bars extend to the full range of results. Anthropogenic and contemporary components are referenced to the 1992–1996 period.

observations in the equatorial Pacific during El Niño events, but not La Niña events. The joint inversion results for air-sea fluxes are driven by ocean interior data which implicitly include the time-averaged effects of interannual variability. Ocean flux interannual variability is dominated by ENSO [*McKinley et al.*, 2003]; during El Niño (La Niña), natural tropical Pacific outgassing is suppressed (enhanced) [*Feely et al.*, 1999]. Averaged over 4–5 years, the effect of El Niño is estimated to represent an anomalous reduction of outgassing of 0.2 PgC yr^{-1} [*Tans et al.*, 1990; *Feely et al.*, 1999]. The difference in tropical Pacific flux estimates between the joint inversion and Tak02, 0.25 PgC yr^{-1}, is consistent with this effect.

[9] Our results suggest that the northern and southern temperate oceans dominate the uptake of atmospheric CO_2, and together are responsible for a contemporary uptake of -2.1 ± 0.2 PgC yr^{-1} (Table 1 and Figure 1). These temperate zones extend from 18°S to 44°S in the Southern Hemisphere, and from 18°N to 49°N in the Atlantic and 66°N in the Pacific. Thus they cover not only the subtropical gyres, but the associated western boundary currents and their extensions, which are areas of intensive seasonal heat loss. The solubility of CO_2 in seawater increases as water cools, so heat loss is closely associated with uptake of carbon dioxide. The high-latitude oceans in both hemispheres are characterized by small uptake, together accounting for -0.35 ± 0.08 PgC yr^{-1}. The extratropical regions together are estimated to have a contemporary air-sea flux of -2.5 ± 0.2 PgC yr^{-1}, opposed by a tropical ocean outgassing of 0.8 ± 0.1 PgC yr^{-1}.

[10] The high-latitude oceans appear to be less of a contemporary sink for CO_2 than is predicted by pCO_2-based estimates, atmospheric inversions, and forward ocean simulations. The Southern Ocean in particular is estimated to have a very small net uptake, with a contemporary air-sea flux of -0.15 ± 0.07 PgC yr^{-1}. This is one quarter the sink

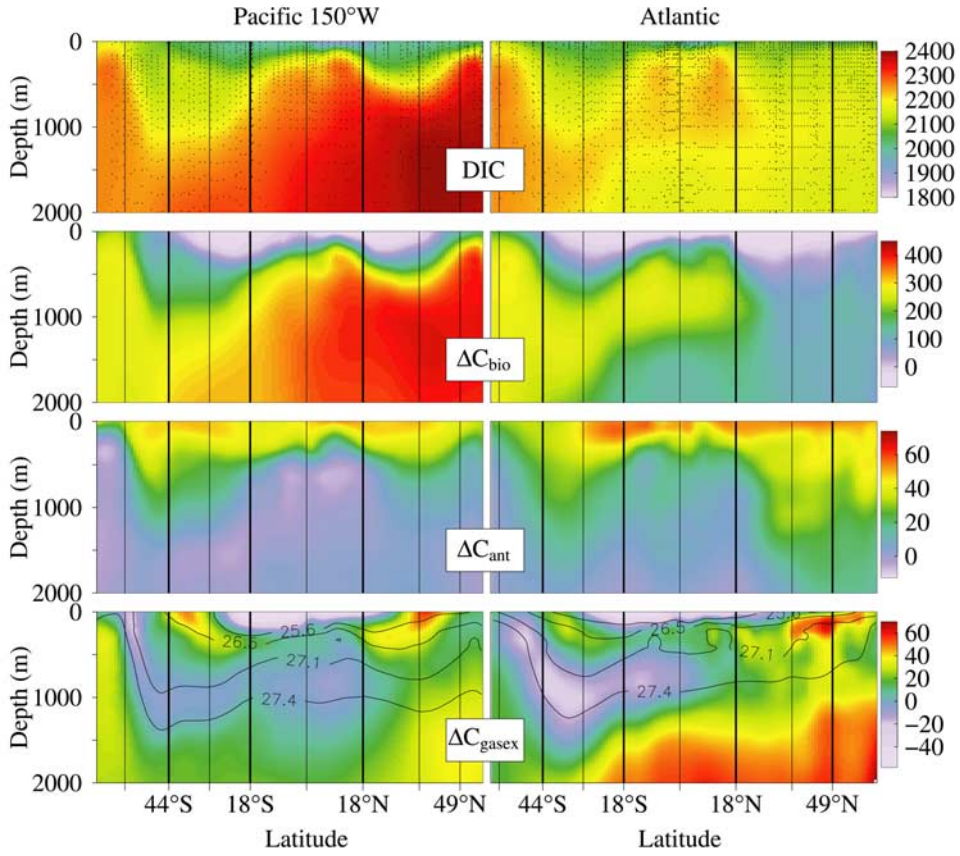

Figure 3. Ocean carbon system components in μmol kg^{-1} along (left) the 150°W section in the Pacific Ocean and (right) along a section in the Atlantic. From top to bottom, the rows represent observed DIC, the biological correction term (ΔC_{bio}), the anthropogenic carbon concentration (C_{ant}), and the preindustrial gas exchange tracer (ΔC_{gasex}). These tracers are defined by *Jacobson et al.* [2007]. Contours of selected isopycnal surfaces (σ_0 in kg m^{-3}) are depicted in the bottom row of panels. The geographic locations of the sections used in this plot are shown in Figure 1 of *Jacobson et al.* [2007]. Thick vertical lines show the TransCom3 regional boundaries and thin vertical lines show the full-resolution regional boundaries used in the oceanic inversion. Black dots in both top panels show the locations of observations from which these fields were interpolated.

size predicted by other methods (Figure 1 and Table 1). In fact, this small contemporary sink is due to large offsetting preindustrial and anthropogenic fluxes (Figure 2). While forward simulations suggest that the oceans south of 44°S were approximately neutral in preindustrial times, the inverse estimates instead predict a preindustrial outgassing of about 0.5 PgC yr^{-1}. This is a significant component of the preindustrial flux budget, with a magnitude about half that of the preindustrial tropical source. However, the Southern Ocean has been subjected to the largest regional anthropogenic perturbation and now comprises a net carbon sink.

[11] The atmospheric inverse estimates of air-sea flux from the TransCom3 studies show significant inconsistencies with findings from surface ocean data, oceanic inversions from interior data, and ocean forward simulations (Figure 1 and Table 1). T3L2 flux estimates suggest ingassing in the tropical Indian ocean and do not detect the expected outgassing from the tropical Atlantic. Taken as a whole, the tropical oceans are estimated by T3L2 to be about neutral, albeit with a large uncertainty. Compared with the other methods, the T3L2 southern temperate basins are either smaller sinks, or in the case of the South Pacific temperate region, a remarkable source. The resulting temperate ocean sink size is only about 28% of the joint inversion estimate. In the extratropical northern oceans, and in the Southern Ocean, the TransCom result is consistent with the Tak02 prediction. The annual mean T3L1 inversion [*Gurney et al.*, 2002] displays similar tendencies, but with generally higher predicted uncertainties.

[12] These inversion results for air-sea fluxes are readily reconciled visually with the carbon tracer observations. Fields of the preindustrial ΔC_{gasex} and anthropogenic ΔC^* tracers (tracer definitions are given by *Jacobson et al.* [2007]) are shown for two representative sections, one in the central Pacific, and the other down the middle of the

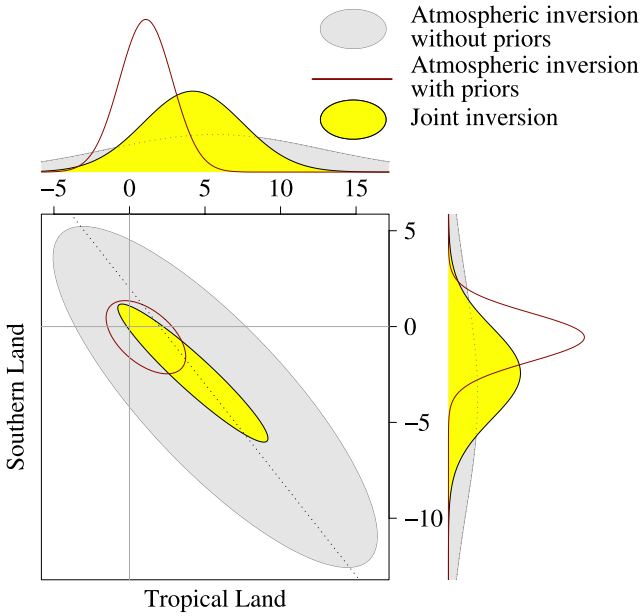

Figure 4. The 68% confidence intervals (ellipses) and marginal probability distributions for aggregated tropical land versus aggregated southern land regions (defined in Table 1) from different inversions, in PgC yr^{-1}. The light grey filled area is a summary of the present unregularized atmospheric inversion, and the yellow filled area depicts the joint inversion result. Red lines are the TransCom3, Level 1 results [*Gurney et al.*, 2002]. The −1:1 slope is shown with a dotted line; ellipses whose major axis is oriented along this line are indicative of negative correlations between the two flux estimates. Narrower ellipses are indicative of stronger correlations than rounder ellipses.

Atlantic ocean, in Figure 3. The observed distributions in the two oceans differ principally owing to the high DIC concentrations in the deep North Pacific. These waters are the oldest in the world oceans, having been out of contact with the atmosphere for more than 800 years [*Broecker and Peng*, 1982] and have accumulated a large amount of remineralized DIC and phosphate. This is reflected in very different ΔC_{bio} fields for the two sections (Figure 3, second row). While anthropogenic carbon (third row) is accumulating in the subtropical gyres, it should be noted that these are not necessarily the latitudes of greatest anthropogenic flux. The deepest penetration of the anthropogenic perturbation is in the deep North Atlantic ocean, where deep wintertime convection associated with the formation of North Atlantic Deep Water provides ventilation of deeper waters, providing a conduit for anthropogenic CO_2 into the ocean interior.

[13] The distribution of ΔC_{gasex} (fourth row of Figure 3) is more complex. While it is surface spatial gradients of ΔC_{gasex} which are directly related to fluxes, large values in the interior generally result from uptake and small values generally are the result of outgassing. The overall pattern indicates that the preindustrial ocean was characterized by tropical outgassing in both basins, a feature associated with meridional mean circulation. The extratropical North Atlantic appears to be characterized by strong preindustrial uptake at mid to high latitudes, but the extratropical South Atlantic suggests uptake just in the 31°S–44°S band corresponding to waters with potential densities greater than about 25.6 and less than 27.1 kg m^{-3} (see bottom row of Figure 3). In contrast, there is significant preindustrial outgassing south of 44°S in the Atlantic in waters with potential densities greater than about 26.5 kg m^{-3}. The Pacific Ocean has a similar pattern to the Atlantic in the Southern Hemisphere, with outgassing in the Southern Ocean between 58°S and 44°S and uptake north of this region. The North Pacific ΔC_{gasex} distribution is dominated by a tongue of positive values apparently resulting from uptake in the 36°N–49°N band.

2.2. Land Fluxes in Detail

[14] Few of the inversion flux estimates for individual land regions are significantly different from zero for any inversion (Figure 3 of *Jacobson et al.* [2007] and Table 1). Land regions in the Northern Hemisphere are generally much more well-constrained than those in the tropics and Southern Hemisphere. In general agreement with previous results, northern boreal land regions in both America and Eurasia are approximately neutral, and temperate land zones are likely sinks of carbon (see Table 1). Of these temperate Northern Hemisphere land regions, only the European sink is significantly different from zero, due not so much to a larger sink size as to a lower uncertainty on the estimate. The northern land sink (−2.9 ± 1.1 PgC yr^{-1}) is due almost entirely to the three temperate regions (−2.8 ± 1.2 PgC yr^{-1}), a finding that does not differ significantly from TransCom results (not shown).

[15] While the South American tropical region is formally estimated to be a significant source, tropical and Southern Hemisphere land regions in general remain very uncertain and display clear evidence of anticorrelated "dipole" behavior. This suggests that estimates for the tropics and Southern Hemisphere land regions should not be considered independently. In Figure 4 we display region-region confidence intervals for the aggregated tropical land regions and southern land regions (TSL; definition given in Table 1). These confidence intervals take the form of ellipsoids whose tilt gives information about dependence between the two flux estimates being plotted. When the major axis of an ellipsoid is tilted toward the −1:1 slope (dotted line), the regional estimates are anticorrelated. In the limit of a very narrow ellipse with major axis along this slope, the two regions cannot be distinguished from one another. The gray ellipse, representing unregularized atmospheric inversion results, clearly displays the southern land versus tropical land dipole. The red ellipse, representing results from an atmospheric inversion using model-based priors, is both smaller and rounder than the gray ellipse, indicating that the priors have acted to deflate the uncertainty and drive the estimates toward independence.

[16] After applying the ocean constraint (joint inversion result shown as a yellow ellipse in Figure 4), terrestrial flux uncertainties are reduced, and we obtain significant flux estimates for each of the two regions: a tropical land

Table 2. Carbon Budget Estimates for Land Regions of the Tropics and Southern Hemisphere[a]

Tropical Land Use Change Source	Residual
0.9 ± 0.5[b]	0.9 ± 1.2
1.1 ± 0.3[c]	0.7 ± 1.1
1.9 (0.7 to 2.5)[d]	-0.1 (-0.7 to 1.3)
2.2 ± 0.8[e]	-0.4 ± 1.3

[a]Units are PgC yr^{-1}. Four estimates of tropical land-use change flux are subtracted from the current study's estimate of the tropical and southern land net flux (1.8 ± 1.1 PgC/yr) to yield a residual flux.
[b]*DeFries et al.* [2002].
[c]*Achard et al.* [2004].
[d]*Food and Agriculture Organization* [2001].
[e]*Houghton* [2003b].

flux which is significantly greater than zero at the 94% probability level, and a southern land flux that is significantly less than zero at the 89% probability level (one-sided probabilities). These results are shown as marginal probability distributions along the sides of Figure 4. However, as indicated by the narrowness and slope of the joint inversion ellipsoid, the southern land and tropical land regions remain strongly anticorrelated, and therefore still cannot be independently estimated.

[17] By computing the aggregate of the strongly anticorrelated tropical land and southern land regions, we arrive at a conclusion about land fluxes that is difficult to see in atmosphere-only inversions. The joint inversion estimates a flux from the aggregated tropical and Southern Hemisphere land of 1.8 ± 1.1 PgC yr^{-1}. This is a significantly larger source than that predicted by the T3L1 and T3L2 inversions, both of which yield 1.0 PgC yr^{-1} with uncertainties of 1.5 and 1.4 PgC yr^{-1} respectively. While the joint inversion implies a 77% probability that these land regions comprise a source of more than 1.0 PgC yr^{-1}, the TransCom3 estimates give only a 49% probability that this is the case. The joint inversion excludes the possibility of the net flux from this region being 0.5 PgC yr^{-1} or less with 88% certainty.

[18] The net tropical and southern land flux we find is the sum of many processes taking place on the ground, including primary production, respiration, land-use change, fire, and potential CO_2 fertilization effects. Process models, field studies, and satellite-based estimates of the net tropical terrestrial carbon flux are currently in disagreement [*Houghton*, 2003a]. There is a particularly strong disparity of estimates for the tropics, due to large differences in estimates of carbon flux due to land use change. Working from AVHRR observations of net forest cover change, *DeFries et al.* [2002] and *Achard et al.* [2004] claim that the tropical land use change source is about 1 PgC yr^{-1} (Table 2). This contrasts with the estimates of $\sim$2 PgC yr^{-1} from studies of the *Food and Agriculture Organization* [2001] and analyses of field studies by *Houghton* [2003b]. While these results indicate that the precise magnitude of the tropical land-use change component remains uncertain, it likely represents a large source of carbon to the atmosphere.

[19] Previous inversions have found that the net tropical land flux is approximately neutral, albeit with a large uncertainty [*Heimann*, 2001]. If this is the case, a tropical land sink of about the same magnitude as the land-use change source is required to explain the inversion results. This has been taken as strong evidence for the existence of a large tropical CO_2 land fertilization sink [*Schimel et al.*, 2001; *Prentice et al.*, 2001]. Terrestrial process models which include CO_2 fertilization and land-use change effects played a major role in the IPCC Third Assessment Report (TAR) [*Prentice et al.*, 2001; *Cramer et al.*, 1999]. Estimates synthesized for the IPCC TAR suggest that a $\sim$2 PgC yr^{-1} fertilization sink was in operation in the early 1990s, and that 45–67% of the expected fertilization sink lies in the tropics, with southern extratropical land playing almost no role whatsoever, owing mainly to its relatively small area [*McGuire et al.*, 2001]. The present finding of a large net source from tropical and Southern Hemisphere land regions challenges the argument for the existence of such a large fertilization sink: While the difference of the joint inversion net source and the deforestation estimates has a large range (Table 2), the implied fertilization effect ranges from a modest sink (-0.4 PgC yr^{-1}) to a sizeable source ($\sim$1 PgC yr^{-1}). Alternatively, the existence of a $\sim$2 PgC yr^{-1} fertilization sink would require a land-use change source of $\sim$4 PgC yr^{-1}, well beyond the upper range of estimates.

[20] Biogeochemical simulations and interannual atmospheric inversions suggest that the Pinatubo eruption in 1992–1993 caused an increased terrestrial sink at high northern latitudes [*Bousquet et al.*, 2000; *Lucht et al.*, 2002]. While our estimation period includes this posteruption time, we see no evidence for anomalous uptake in the northern boreal regions (Table 1). If an increase in diffuse radiation or decrease in surface temperatures caused increased production in lower latitude terrestrial ecosystems, the magnitude of any fertilization sink estimated as a residual from our results would have to be reduced by a similar amount.

[21] The carbon cycle of the tropical forest ecosystems of the Amazon basin in South America has been extensively studied. This region is an important contributor to the tropical and southern land flux result we obtain, so observational estimates of carbon exchange in the Amazon are directly relevant to evaluating our results. While the carbon balance of Amazonian forests remains highly uncertain, recent direct observational estimates using eddy flux covariance methods, forest inventories, and boundary layer budgeting based on aircraft observations, suggest that these forests may not be a large sink of carbon. Earlier reports based on eddy flux covariance methods concluded that Amazonian forests are a sink on the order of 4–5 PgC yr^{-1} [*Malhi et al.*, 1998; *Andreae et al.*, 2002]. However, as shown by *Miller et al.* [2004], the inability of eddy flux covariance techniques to capture fluxes in the absence of turbulent flow can result in a large bias. Plant respiration occurring during calm periods, especially at night when advective drainage flows can transport carbon laterally to pool in low areas, can account for an offsetting carbon release of about the same magnitude, 4–5 PgC yr^{-1}, as the sink estimated

by the earlier studies [*Miller et al.*, 2004]. This bias is particularly large for tropical forests, since they are characterized by respiration throughout the entire year, as opposed to mid- and high-latitude forests which have more seasonally intermittent respiration. Forest inventories, meanwhile, indicate that while there have been substantial changes in ecosystem composition and function for intact old-growth forests, the carbon uptake implied by these changes is only on the order of 0.6 PgC yr^{-1} [*Phillips et al.*, 2002; *Baker et al.*, 2004]. Finally, boundary layer carbon budgets constructed using aircraft vertical profile measurements of CO_2, CO, and O_3 during April and May 1987 at Manaus (Brazil) lead *Chou et al.* [2002] to conclude that a substantial fraction of the Amazon was in balance during this period.

3. Why Have Others Not Detected a Large Tropical Land Source?

[22] Atmospheric inversion analyses are subject to lingering questions about sensitivity to details of methodology [*Fan et al.*, 1999; *Kaminski et al.*, 2001; *Engelen et al.*, 2002], to the inclusion of more data as the GlobalView CO_2 monitoring network grows [*Rödenbeck et al.*, 2003a], to the nonconservation of atmospheric CO_2 [*Enting and Mansbridge*, 1991], and to the uncertain modeling of atmospheric transport [*Gurney et al.*, 2002, 2003]. These uncertainties and biases are strongly exacerbated by the severely underdetermined nature of the atmospheric inverse problem. Nevertheless, given the substantial history of atmospheric inversion research, it is reasonable to ask how such a significant terrestrial source in the tropical and Southern Hemisphere could have gone undetected until now.

[23] It is convenient to compare our results with those of TransCom3 (T3L1 and T3L2) to address this question. There are three reasons that may explain why the present study detects a tropical and southern land source. The first, and most important, is that ocean interior and atmospheric data have never before been combined in a joint inversion framework. Atmospheric inversions have generally applied ΔpCO_2-based estimates of air-sea fluxes as loose but regionally independent prior constraints (but see *Fan et al.* [1998]). There exist potential biases in ΔpCO_2-based estimates, such as the spatial and temporal extrapolation of pCO_2 observations and the application of uncertain bulk parameterizations of gas exchange, which could induce spatially coherent errors in the flux estimates. In large regions of the Southern Hemisphere, the pCO_2 data set is quite sparse and subject to seasonal sampling biases. In addition, tropical Pacific air-sea fluxes from the Tak99 and Tak02 estimates are biased toward excessive outgassing since those products exclude observations from El Niño years and include those from La Niña years. In contrast, the ocean interior data used in this study contain a low-pass filtered record of air-sea gas exchange over the entire anthropocene, including the average ENSO state. The two constraints on air-sea fluxes also have differing strengths. In the joint inversion, oceanic estimates of air-sea flux dominate the corresponding atmospheric estimates, whereas the Tak99 priors were applied rather loosely in T3L1 and T3L2 [*Gurney et al.*, 2003], such that the final results from those studies appear to reject the ΔpCO_2-based estimates for many regions in the tropics and Southern Hemisphere (Figure 1). The ocean models used in this study have been extensively evaluated by comparing with observed physical, biological, and carbon system tracer distributions [*Orr et al.*, 2001; *Gnanadesikan et al.*, 2004; *Matsumoto et al.*, 2004]. The ocean interior data are also well-distributed spatially (Figure 1 of *Jacobson et al.* [2007]), and, importantly, extend vertically throughout the water column (Figure 3).

[24] The second reason for our finding of a large source from the tropical and southern land is that we are considering different regional aggregates than previous studies. As shown in Figure 4, the tropical and southern land flux estimates remain tightly anticorrelated despite the use of ocean inversion air-sea fluxes. We have used the off-diagonal elements of the flux covariance matrix to diagnose regions that cannot be distinguished from one another, and report results for their aggregate. Our use of inversion without regularization at 22-region resolution followed by post-hoc aggregation allows us to obtain a flux estimate for the very large TSL region while avoiding further preaggregation bias. The alternative of inverting for the TSL flux as one large region would expose us to a significant risk of large region bias [*Kaminski et al.*, 2001].

[25] The third reason is that we do not use regularization techniques and thus avoid biases associated with those methods. Naturally, the imposition of priors drives the solution toward those prior values. However, for this application it is the imposition of priors as independent regional flux estimates that is called into question. The independence of the prior fluxes translates directly through the matrix inversion to increase the independence of flux estimates. This increases the effective number of independent parameters, which has a side effect of discouraging multiple regions from having excursions of similar signs.

[26] We have conducted a limited synthetic data experiment to numerically demonstrate the ability of ocean data to reliably detect anomalies in poorly constrained land regions. The "truth" condition for this exercise is a stochastically chosen set of regional fluxes which are propagated through an atmospheric transport model selected at random from the set of 16 available simulations. The noiseless synthetic data thus derived are then inverted following the methods described by *Jacobson et al.* [2007]. Separate atmospheric inversions are performed first, without regularization or an ocean flux presubtraction, using each of the transport models. These estimates are then combined with the 10 real ocean inversion flux estimates using the joint inversion methodology. This is not a test of the ocean inversion, as only atmospheric data are being simulated. As a result, the truth condition has air-sea fluxes similar to the ocean inversion fluxes. The probability distribution we used for the truth condition has independent fluxes for all land and ocean regions. Land region fluxes are each distributed normally about zero with a standard deviation of 1 PgC yr^{-1}, and ocean region fluxes are distributed normally about the ocean inversion central estimate, but with a variance that is twice

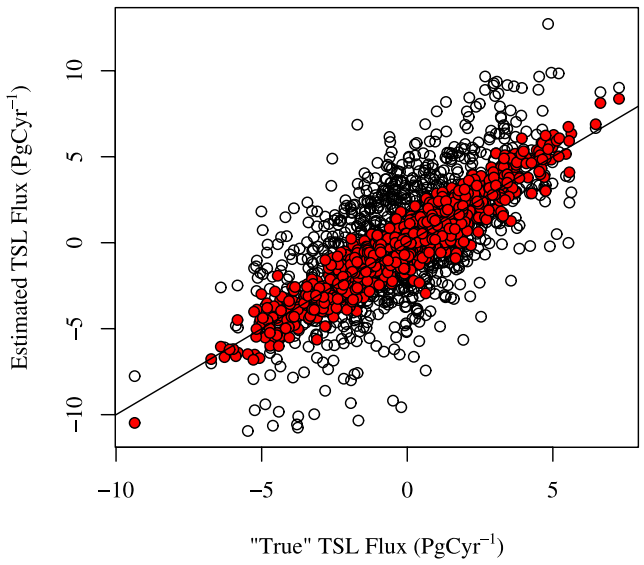

Figure 5. Performance of atmospheric (open circles) and joint (filled red circles) inversions at estimating tropical and southern land (TSL) fluxes in a synthetic data exercise (section 3). The synthetic flux distribution is normally distributed about zero with standard deviation $\sqrt{5}$ PgC yr^{-1}.

the actual estimate. This truth condition disadvantages the ocean constraint by allowing synthetic air-sea fluxes that are larger than those of the ocean inversion, and that are distributed independently. This exercise is repeated 1,000 times with different synthetic fluxes, and we consider the deviations of estimated from "true" fluxes for poorly constrained land regions.

[27] We find that root mean square flux errors for the tropical and southern land regions (TSL) are 2.9 PgC yr^{-1} for the atmospheric inversion alone, and 0.8 PgC yr^{-1} for the joint inversion (Figure 5). The TSL fluxes estimated by the joint inversion capture 90% of the variance in the "true" fluxes, whereas the atmospheric inversions alone only capture 38% of this variance. These results show the power of accurate air-sea fluxes to properly constrain terrestrial fluxes in underobserved regions.

[28] The study of *Rödenbeck et al.* [2003b] (henceforth, RHGH) is an apparent exception to the above reasoning. Those authors used the ocean inversion fluxes of *Gloor et al.* [2003] as priors in an atmospheric inversion, but found that the tropics were a significant sink of carbon. There are significant differences between the atmospheric inversion methods of RHGH and those used in the present study, perhaps the most fundamental of which is that the RHGH inversion is focused on estimating interannually varying fluxes. The authors of that study take care to state that the spatial distribution of long-term fluxes cannot be estimated as reliably as temporal variability of fluxes, a conclusion based on concerns about the underdeterminacy of the spatial part of the inverse problem.

[29] The temporally invariant inversion of the present study requires the simulation of the background "rectifier" field, which owes its existence to seasonal covariations of surface flux and atmospheric circulation [*Denning et al.*, 1995]. Rectifier field estimates are computed by propagating assumed fixed seasonal cycles of biosphere exchange through a transport model. The seasonal cycles in RHGH are allowed to vary and the inversion is thus presumably free of rectifier biases, but at the cost of having to estimate more fluxes. While RHGH is a single-model analysis, the present study takes advantage of 16 different atmospheric simulations, so transport biases, including those involved in computing the rectifier field, are considered. A major difference between T3L1 and T3L2 is that the latter study did not require the estimation of a seasonal rectifier field. The differences between those two studies are small compared with the TSL signal we report.

[30] One potential cause for discrepancies between the present results and those of RHGH is that in that study, ocean inversion fluxes are applied as priors in a manner which does not respect the ocean inversion's inherent uncertainty structure. The high spatial resolution of RHGH is maintained by enforcing spatial correlations between grid boxes, which reduces the effective number of free parameters while mitigating the effects of spatial aggregation bias. To establish uncertainties on the priors, the regional uncertainties reported by *Gloor et al.* [2003] are distributed among the ocean grid boxes, then scaled up so that their sum matches the reported global uncertainty of 0.4 PgC yr^{-1}. The flux priors are then assumed to decorrelate isotropically with a length scale of 1912 km. This effectively abandons the between-region correlations in ocean inversion flux estimates and allows the atmospheric inversion to adjust its fluxes in a manner inconsistent with the ocean inversion. The *Gloor et al.* [2003] fluxes also have no seasonal variability, so the annual mean flux prior must be distributed among the months using presumed temporal variability. Finally, it should be recognized that the *Gloor et al.* [2003] global flux uncertainty is significantly larger than the current study's ±0.22 PgC yr^{-1}, which permits correspondingly large deviations from the prior values.

4. Sensitivity Tests

[31] Our finding of a large flux source in the tropical and southern land (TSL) regions is driven principally by the use of air-sea fluxes from the ocean inversion. Air-sea fluxes integrated across the tropics and Southern Hemisphere from T3L2, Tak02, forward simulations, and ocean inversions are in agreement to within ±0.3 PgC yr^{-1}. To explain an increase in the TSL flux of ∼0.8 PgC yr^{-1} over T3L2, we must therefore look beyond the total hemispheric air-sea flux to the spatial distribution of that flux within the Southern Hemisphere. Relative to forward simulations and ΔpCO_2-based estimates, the ocean inversion predicts less uptake in the contemporary Southern Ocean and more uptake in the southern temperate latitudes (Figure 1). Tropical ocean outgassing estimated by the ocean inversion is in agreement with forward models, and the disagreement

with ΔpCO_2-based estimates is consistent with the Tak02 exclusion of El Niño years. In what follows, we show the following: (1) that the TSL source cannot be detected by using Tak02 fluxes; (2) that the TSL source can be explained by reallocating ocean uptake between the temperate and high latitudes; (3) that the TSL source is not due to known biases in ΔC^*, to inaccurate estimates of the atmospheric CO_2 growth rate, or to the assumption of surface oxidation of reduced carbon compounds generated during combustion and biospheric exchange; and (4) that the TSL source can be attributed to ocean inversion estimates of preindustrial Southern Ocean fluxes that differ from ΔpCO_2-based estimates and forward simulations. We conclude with a discussion of what might drive these differences in preindustrial Southern Ocean flux estimates.

[32] One possible explanation for observed differences is that ΔpCO_2-based fluxes used as priors in previous atmospheric inversions were applied too loosely. To test this possibility, we conducted a joint inversion in which air-sea fluxes from Tak02 were applied in the place of ocean inversion fluxes. These ΔpCO_2 fluxes were given the tight uncertainties of the ocean inversion fluxes, ± 0.22 PgC yr^{-1} globally, with the uncertainty for each region proportional to the ΔpCO_2-based flux and independent from other regions. The resulting TSL flux estimate is not distinct from zero (0.8 ± 1.1), indicating that the looseness of the imposed ΔpCO_2 flux priors is not to blame for missed detection of the TSL source in previous inversions.

[33] The salient difference between our ocean inversion fluxes and estimates from forward models and ΔpCO_2 analysis is that the present results have stronger southern temperate and weaker high southern uptake (Figure 1). To determine whether this difference is responsible for an increased TSL source, we artificially reallocated 0.4 PgC yr^{-1} of uptake from the southern temperate latitudes to the Southern Ocean. This brings the temperate flux down to -0.9 PgC yr^{-1} and the Southern Ocean flux up to -0.5 PgC yr^{-1}, both of which are consistent with ΔpCO_2-based estimates and forward simulations. In this sensitivity test, the TSL source is significantly reduced, from 1.8 ± 1.1 PgC yr^{-1} to 1.2 ± 1.1 PgC yr^{-1}. This indicates that the partitioning of the Southern Hemisphere air-sea flux between the Southern Ocean (<44°S) and the southern temperate latitudes (18°S–44°S) is critical for constraining the TSL flux.

[34] Using synthetic data derived from a forward biogeochemical simulation, *Matsumoto and Gruber* [2005] have quantified the effects of some biases in the C* method for estimating anthropogenic carbon concentrations. These biases arise from three sources: (1) the assumption that air-sea disequilibrium in each location has remained constant; (2) an age bias due to mixing effects when considering *p*CFC ventilation; and (3) errors in decomposing a given sample into contributions from uniquely identifiable water masses. Initial results suggest that the global inventory of anthropogenic carbon may be overestimated by 7% owing to these biases. We have attempted to account for these biases in both preindustrial and anthropogenic inversions, using a provisional model of the spatial distribution of this bias [*Mikaloff Fletcher et al.*, 2006]. While biases that increase C_{ant} tend to decrease the preindustrial carbon tracer ΔC_{gasex}, the relative change is greater for the anthropogenic tracer. As a result, the correction favors reducing the estimated ocean sink, which becomes smaller by about 0.17 PgC yr^{-1} in the process. The error estimates for regional fluxes are also increased by this correction, by assuming that the uncertainty in quantifying the bias has a standard deviation that is 100% of the bias estimate itself. The effect of this bias correction is to decrease southern temperate uptake by about 0.1 PgC yr^{-1}, but the change in Southern Ocean uptake is negligible. The reduction of the global ocean sink requires that the global land sink increase by a similar amount. Unsurprisingly, 77% of this correction is absorbed by the TSL regions. Nonetheless, the final TSL flux is still significantly larger than zero (1.6 ± 1.1 PgC yr^{-1}), so we conclude that the TSL flux result is robust with regard to these identified biases.

[35] While our estimate of global air-sea flux is tightly constrained by the oceanic data, the magnitude of the global land sink is only set by applying the difference between the observed atmospheric growth rate and fossil fuel consumption estimates as a mass balance constraint. This mass balance constraint would not be necessary if there were sufficient atmospheric observations, because if the regional fluxes were all accurately estimated, the global total would also be well constrained. In the present case the atmospheric inverse problem remains strongly underconstrained, and the mass balance constraint is useful. We use the 1992–1996 atmospheric burden growth rate established by TransCom3 (3.27 PgC yr^{-1}), but this number is subject to methodological uncertainty. The atmospheric growth rate is also highly variable in time, but the period in question is relatively free of anomalous interannual variability. A linear least squares fit to low-pass filtered Mauna Loa time series during the period 1992–1996 gives a growth rate of 3.31 PgC yr^{-1}, but if the same filtered time series is sequentially differenced to make a time series of growth rates, its average during the same period is 2.95 PgC yr^{-1}. We believe that the former method is statistically consistent with estimating the long-term mean fluxes. Nevertheless, we performed a set of inversions using the lower growth rate estimate, and as in the previous sensitivity test, this resulted in an adjustment of the least-well-constrained terrestrial fluxes, those of the tropics and Southern Hemisphere. Using the lower growth rate, the global land sink grows to take on the difference. The tropical land source is reduced moderately, by 0.25 PgC yr^{-1}, and effects on uncertainties and on fluxes for other regions are negligible.

[36] The nonconservation of atmospheric CO_2 due to oxidation of reduced carbon species such as carbon monoxide is a potential source of bias in our conclusion of a southern land source [*Enting and Mansbridge*, 1991; *Baker*, 2001]. CO is produced by incomplete combustion on land, and has an atmospheric lifetime of 1–2 months, during which time it can be transported to another location before being oxidized to CO_2. Considering the oxidation source of CO_2 therefore acts to increase the extent of a region's atmospheric footprint, by decreasing the footprint concentration directly over the flux region, and increasing it remotely. This tends to extend the footprint of Northern

Hemisphere fossil fuel and biospheric fluxes toward the south, allowing the inversion to attribute some of the CO_2 observed in the atmosphere at stations in tropical and southern latitudes to remote northern sources, instead of to local sources. Accounting for reduced carbon can therefore be expected to reduce the size of the northern terrestrial sinks and decrease the size of the tropical source. *Baker* [2001] estimates that a maximum global CO_2 source is on the order of 0.2 PgC yr^{-1}, but in that study CO was eventually oxidized at similar latitudes to its production, and thus had a minor impact on flux estimates. Recently, *Suntharalingam et al.* [2005] have completed an atmospheric chemistry simulation estimating the impact of oxidation of CH_4 and CO on the atmospheric fossil fuel and neutral biosphere presubtraction fields used in the TransCom3 atmospheric inversion (see details in work by *Jacobson et al.* [2007]). We have conducted a joint inversion in which these corrected presubtraction fields were used. As expected, flux is reallocated from the tropical and southern land source to the Northern Hemisphere in this correction. The northern land sinks become smaller by 0.3 PgC yr^{-1}, and the TSL source decreases by an equivalent amount to 1.4 ± 1.1 PgC yr^{-1}.

5. Preindustrial Southern Ocean Flux Sensitivities

[37] Ocean inversion estimates of anthropogenic flux in the Southern Hemisphere do not disagree substantially with forward simulations (Figure 2, top). In the Southern Ocean, there are intriguing differences between inversions using different surface flux patterns, with the Tak02-pattern inversions suggesting enhanced anthropogenic carbon uptake. Preindustrial flux estimates, however, show marked differences in the Southern Ocean, where inversions robustly predict a preindustrial outgassing of about 0.5 PgC yr^{-1}, and forward simulations suggest that this region was approximately neutral in preindustrial times (Figure 2, middle). Analysis of the ocean inversion results at their full resolution (27 regions, with twice the number of latitude bands) shows that preindustrial outgassing was principally restricted to the subpolar band north of 58°S. The pattern of alternating preindustrial outgassing south of 44°S and preindustrial uptake north of this latitude is also strongly suggested by the ΔC_{gasex} fields shown in Figure 3, in which low values are characteristic of outgassing, and high values characteristic of uptake. That there should be a strong preindustrial outgassing in this 58°S–44°S band seems reasonable given that this is the region where circumpolar deep water upwells, with its large load of DIC. The preindustrial uptake north of 44°S, conversely, is likely associated with the "solubility pump." This is an effect of the cooling of subtropical waters as they move poleward, in which CO_2 is taken up owing to its increasing solubility with decreasing water temperature. Owing to the sensitivity of our terrestrial flux results on this single feature of the oceanic inversions, we now consider possible reasons that forward and inverse simulations differ in this manner.

[38] Transport uncertainty is unlikely to explain the observed discrepancy. The suite of ocean models used for this study was specifically conceived to study Southern Ocean processes [*Gnanadesikan and Hallberg*, 2000]. The five model configurations span a broad range of possible circulation and ventilation schemes for the Southern Ocean, with each one striking a different balance in the means by which dense water is converted to light water. In the *Gnanadesikan and Hallberg* [2000] pycnocline theory, the balance between density conversion in the low latitudes and the Southern Ocean is set by systematically varying vertical and along-isopycnal diffusivities in the circulation model, while taking care to preserve the same overall density structure. These model configurations have very significant differences in Southern Ocean upwelling and circulation (see Southern Ocean watermass transformation rates in Table 1 of *Jacobson et al.* [2007]), and thus it is very unlikely that they all possess a similar circulation bias that could lead to a bias in the inverted preindustrial fluxes. Given that the same circulation configurations are used in both forward and inverse computations, we are left with only two possible explanations for the discrepancy: either the C* decomposition is biased, or the forward simulations are biased.

[39] The oceanic inversion is very stable owing to the large number and relatively even spatial distribution of observations used to constrain a small number of regional fluxes. Since as we argue above, uncertainty in simulated transport is an unlikely candidate to explain our preindustrial inversion result for the mid and high latitudes of the Southern Hemisphere, we conclude that it is driven primarily by the data. In fact, the ΔC_{gasex} distribution shown in Figure 3 reveals clearly the evidence for our results: Strong preindustrial outgassing in the 58°S–44°S band is related to lower values of ΔC_{gasex}, and preindustrial uptake north of this region in the 44°S–31°S band is associated with higher values of ΔC_{gasex}. These patterns of ΔC_{gasex} are consistent with our understanding of the Southern Ocean circulation, and in what follows we discuss their likely oceanographic origins. We then assess whether uncertainties and biases in the computation of ΔC_{gasex} could have a significant impact on our conclusions.

[40] In the high southern latitudes south of 58°S, circumpolar deep water (CDW) upwells to the surface with moderately elevated values of ΔC_{gasex} ($\sim$30 μmol kg^{-1}). Some of this water is moved equatorward by wind-driven surface transport. As a result of the upwelling and subsequent surface transport, these waters are warmed, made less salty, and mixed with surface water, reducing their densities to between 27.1 and 27.4 kg m^{-3}, characteristic of the intermediate waters they will eventually form. By the time these waters leave the surface ocean, they have ΔC_{gasex} values of ~ -40 μmol kg^{-1}, implying a ΔC_{gasex} gradient between the freshly upwelled CDW and the source waters for intermediate waters of 60 to 70 μmol kg^{-1}. This means that each m^3 of water in this meridional mean overturning circulation in the Southern Ocean loses 60 to 70 mmol of CO_2 to the atmosphere while it is at the surface in the 58°S–44°S band. This outgassing is in major part due to the inefficiency of biology in the Southern Ocean, which is manifested in high surface nutrient concentrations [*Sigman and Boyle*, 2000; *Sarmiento et al.*, 2004]. More efficient

biological production would strip DIC from the surface waters, thereby reducing outgassing.

[41] Similarly, the strong natural uptake of CO_2 in the 44°S–31°S band revealed by Figure 3 is driven by the concentration gradient between lower latitude surface waters containing ΔC_{gasex} concentrations below -40 μmol kg^{-1} and the surface waters in the 44°S–31°S band characterized by ΔC_{gasex} concentrations as high as 50 μmol kg^{-1}. Low-latitude waters are transported poleward in the wind-driven surface circulation, during which time they can take up a substantial amount of CO_2 from the atmosphere to compensate both for increased solubility due to cooling, and for biological drawdown of DIC. In this process, their ΔC_{gasex} concentration increases by up to 90 μmol kg^{-1}.

[42] These conclusions could not be supported if biases in ΔC_{gasex} between the different water masses could explain the observed gradients. For example, if ΔC_{gasex} estimates were biased low in the subpolar band (58°S–44°S), and biased high in the 44°S–31°S and 80°S–to 58°S bands, the surface ΔC_{gasex} distribution would be more uniform. This would result in smaller preindustrial fluxes estimated by the inversion. Since ΔC_{gasex} is essentially a residual of the observed DIC after removing the C_{ant} and ΔC_{bio} components [see *Jacobson et al.*, 2007, equation [4]], we must consider errors in both of these fields to assess potential biases.

[43] A systematic overestimation of C_{ant} in the subpolar band and a systematic underestimation in the 44°S–31°S and 80°S–58°S bands could explain the observed ΔC_{gasex} gradients. However, the surface ΔC_{gasex} difference between these two latitude bands is 60–70 μmol kg^{-1} (Figure 3), so the C_{ant} bias would need to be larger than the highest possible anthropogenic CO_2 concentration estimate (Figure 3). Although the Southern Ocean is perhaps the most difficult location for determining C_{ant} primarily because of the uncertainties associated with the estimation of preformed concentrations of oxygen and CFCs, there is no indication that the uncertainty in C_{ant} in this region exceeds 20%, or maximally about 15 μmol kg^{-1}. More importantly, the tongue of negative ΔC_{gasex} responsible for the subpolar outgassing flux extends to about 1500 m, well below the level of significant anthropogenic carbon penetration in the Southern Hemisphere. Similarly, the tongue of positive ΔC_{gasex} extending from the 44°S–31°S band is a bit deeper and more sharply localized than the C_{ant} estimate. It therefore would be difficult to erase the estimated ΔC_{gasex} gradients by reasonable changes in the C_{ant} distribution. Doing so would also require that the inversion estimates of anthropogenic fluxes, which are currently consistent with forward simulations, undergo significant changes.

[44] A more likely candidate for causing biases in ΔC_{gasex} is errors in the biological correction, ΔC_{bio}. Since the magnitude of ΔC_{bio} in the critical latitude bands is as large as 300 μmol kg^{-1}, systematic changes in the stoichiometric ratios of the order of 20% could erase the 50 to 100 μmol kg^{-1} gradients in ΔC_{gasex}. While one cannot exclude stoichiometric ratio biases of this magnitude, there are several arguments supporting our interpretation that the variations in ΔC_{gasex} shown in Figure 3 are real and not artifacts of biases in the assumed ratios.

[45] Perhaps the most important argument is the very good agreement between the expected and exhibited nearly conservative behavior of ΔC_{gasex} away from the surface. By definition, ΔC_{gasex} can be altered at the surface by exchanging CO_2 with the atmosphere, but in the ocean's interior, only mixing can alter its concentration. The pattern of ΔC_{gasex} in Figure 3 follows water masses as delineated by the isopycnals, with intermediate waters clearly marked by a minimum in ΔC_{gasex} and the CDW and the upper ocean mode waters marked by ΔC_{gasex} maxima. If this pattern were an artifact of a bias in ΔC_{bio}, the stoichiometric ratio of phosphorus to carbon in remineralized organic matter would have to vary substantially between water masses. This is unlikely since the factors known to influence remineralization processes are mostly set at the surface, such as initial composition of the organic matter and ballast content, whereas the primary factor known to influence remineralization once organic matter leaves the surface is depth.

[46] The spatial variability in stoichiometric ratio required to erase the ΔC_{gasex} gradients can be illustrated by contrasting the ΔC_{gasex} signals at ~1500 m between the 80°S–58°S band and 58°S–44°S latitude bands in the Pacific 150°W section (Figure 3, left). At these depths, the phosphate concentration between the two bands is relatively similar, resulting in a similar magnitude of ΔC_{bio} of about 250 μmol kg^{-1} (the contribution of $CaCO_3$ changes to ΔC_{bio} is much smaller and not considered here). If lateral variations in plankton stoichiometry are to explain the 50 to 60 μmol kg^{-1} difference in ΔC_{gasex} in these middepth waters, the C:P ratio in the 58°S–44°S would have to be about 25% lower than in the 80°S–58°S band. Nearer the surface at about 500 m, however, the lateral ΔC_{gasex} gradient remains similar to that at middepth, whereas ΔC_{bio} is quite different between the two bands, only on the order of 100 μmol kg^{-1} to the north. In order to explain the lateral ΔC_{gasex} gradient in the shallower waters, the C:P ratio in the 58°S–44°S would have to be about 50% lower than in the 80°S–58°S band. This would require that the C:P ratio increase very strongly with depth in the 58°S–44°S band, but remain nearly constant with depth in the 80°S–58°S band.

[47] An even more striking example is the 44°S–31°S latitude band, where the elimination of the vertical ΔC_{gasex} pattern would require a C:P ratio that is extremely large near the surface (more than twice the canonical value), has a minimum at middepth and has intermediate values in the deep ocean. Observations of C:P ratios in sediment traps do not show such a behavior (see, e.g., the recent summary by *Schneider et al.* [2003]).

[48] Thus, while there exist nonnegligible uncertainties in the inferred distribution of ΔC_{gasex}, our current understanding of possible variations in remineralization stoichiometry suggests that the ΔC_{gasex} distribution in the Southern Hemisphere is quite robust. Nevertheless, improved estimates of stoichiometric ratios based on water column chemistry and sediment trap analysis would help to better constrain our interpretation of ΔC_{gasex}.

[49] Another possible explanation for the discrepancy is that the forward simulations have incorrectly modeled the preindustrial carbon cycle. As demonstrated by *Murnane et*

al. [1999], Southern Ocean fluxes are the result of a small imbalance between two large pumps: The effect of the worldwide biological carbon pump is to drive outgassing in the Southern Ocean, whereas the solubility pump has the opposite effect. Our inversion results are therefore consistent with forward models either underestimating the magnitude of the biological pump, or overestimating the effects of the solubility pump. Consistent with the finding of *Murnane et al.* [1999], preindustrial Southern Ocean (south of 44°S) carbon fluxes in the OCMIP2 simulations of these models are quite sensitive to the inclusion of biology: Whereas the "biotic" simulations are approximately neutral, the "abiotic" versions predict a Southern Ocean uptake of about 0.5 to 1.0 PgC yr^{-1}. In the OCMIP2 biotic protocol, biological net primary production is diagnosed by restoring to observations of surface phosphate. The magnitude of the biological pump could be underestimated by this scheme if the estimated surface phosphate is too low, as could result from a summertime observational bias.

[50] An interesting result pointed out by *Murnane et al.* [1999] and reinforced recently by *Doney et al.* [2004] is the tendency of models to underestimate the northward transport of heat in the Atlantic Ocean. This is likely to be representative of a meridional overturning circulation which is too weak in the Atlantic. The North Atlantic Deep Water formation in the current models is about 12 Sv [*Jacobson et al.*, 2007, Table 1], which is on the low end of the OCMIP2 range [*Doney et al.*, 2004]. A bias toward weak Atlantic overturning would tend to reduce the southward interhemispheric flow of DIC carried by North Atlantic Deep Water. Much of this DIC load is thought to be released in the Southern Ocean where it upwells as Circumpolar Deep Water. Thus a bias toward too little overturning in the Atlantic is consistent with forward simulations predicting too little preindustrial outgassing in the Southern Ocean.

[51] The strong underdetermination of the annual mean atmospheric inverse problem is highlighted by these sensitivity tests. While air-sea fluxes are subject to small, predictable changes due to the potential sources of bias we have considered, the overall pattern of contemporary ocean fluxes predicted by the oceanic inversion is quite robust. Terrestrial fluxes are more sensitive to these biases, especially in the underconstrained regions of the tropics and Southern Hemisphere. The TSL source estimate inherits most of the uncertainty due to potential biases, since it is essentially a residual after accounting for air-sea flux and fluxes from the relatively well-constrained northern land regions. Modeling the emission of reduced carbon, imposing smaller atmospheric growth rate estimates, and considering potential oceanic C_{ant} biases all act to reduce the statistical significance of the TSL source result. For this reason, we believe it is vital to robustly quantify the uncertainty in our results. From this point of view it is important to note that the uncertainties we report here are a raw expression of the limitations of the atmospheric inversion, and have not been artificially reduced by using regularization techniques (see auxiliary material[1] for details). At the same time, they are still likely to underestimate the full uncertainty, as we have only included those uncertainties which could be quantified and therefore used in a formal error analysis. There also remains a risk of bias in these results due to the use of large flux regions [*Kaminski et al.*, 2001].

[1]Auxiliary material data sets are available at ftp://ftp.agu.org/apend/gb/2006gb002703. Other auxiliary material files are in the HTML.

6. Conclusions

[52] The major findings from this study are the following.

[53] 1. Tropical land was a source of carbon dioxide in this period, and the extratropical Southern Hemisphere land was a sink. Fluxes for these regions cannot be reliably estimated independently, but their aggregate is well constrained. Together, the tropical and southern land regions were a source of 1.8 ± 1.1 PgC yr^{-1} over the period 1992–1996, corresponding to a 77% probability that this source exceeded 1.0 PgC yr^{-1}.

[54] 2. After subtracting a tropical land-use change source of 1–2 PgC yr^{-1} from the estimated net tropical and southern land flux, a residual flux of between about -0.4–0.9 PgC yr^{-1} remains. The terrestrial CO_2 fertilization sink is contained in this residual, and these results imply that a large fertilization sink is unlikely.

[55] 3. The air-sea flux pattern including both preindustrial and anthropogenic fluxes shows strong temperate uptake. High-latitude uptake, especially in the Southern Ocean, is weaker than is predicted by forward simulations, atmospheric inverse modeling, and ΔpCO_2-based methods. The finding of a large terrestrial and southern land source of CO_2 is strongly driven by this spatial distribution of air-sea flux in the Southern Hemisphere.

[56] **Acknowledgments.** Jacobson, Sarmiento, and Gloor were supported by an award from the National Oceanic and Atmospheric Administration, U.S. Department of Commerce, and by the Carbon Mitigation Initiative, with support provided by BP Amoco and the Ford Motor Company. Gruber and Mikaloff Fletcher were supported by a grant from the National Aeronautics and Space Administration. The present analysis would not be possible without the observational data provided by countless oceanographers participating in the WOCE/JGOFS campaign and atmospheric scientists participating in the Globalview-CO_2 program. We thank Steve Pacala, Robbie Toggweiler, and five anonymous reviewers for helpful suggestions on an earlier draft of this paper. TransCom modelers are K. R. Gurney, R. M. Law, A. S. Denning, P. J. Rayner, D. Baker, P. Bousquet, L. Bruhwiler, Y.-H. Chen, P. Ciais, S.-M. Fan, I. Fung, M. Gloor, M. Heimann, K. Higuchi, J. John, T. Maki, S. Maksyutov, P. Peylin, M. Prather, B. C. Pak, J. L. Sarmiento, S. Taguchi, T. Takahashi, and C.-W. Yuen. TransCom results were made possible through support from the National Science Foundation (OCE-9900310), the National Oceanic and Atmospheric Administration (NA67RJ0152, Amend 30) and the International Geosphere Biosphere Program/Global Analysis, Interpretation, and Modeling Project. The statements, findings, conclusions, and recommendations are those of the authors and do not necessarily reflect the views of the National Oceanic and Atmospheric Administration, or the U.S. Department of Commerce.

References

Achard, F., H. D. Eva, P. Mayaux, H. J. Stibig, and A. Belward (2004), Improved estimates of net carbon emissions from land cover change in the tropics for the 1990s, *Global Biogeochem. Cycles*, *18*, GB2008, doi:10.1029/2003GB002142.

Andreae, M. O., et al. (2002), Biogeochemical cycling of carbon, water, energy, trace gases, and aerosols in Amazonia: The LBA-EUSTACH experiments, *J. Geophys. Res.*, *107*(D20), 8066, doi:10.1029/2001JD000524.

Baker, D. F. (2001), Sources and sinks of atmospheric CO_2 estimated from batch least-squares inversions of CO_2 concentration measurements, Ph.D. thesis, Princeton Univ., Princeton, N. J.

Baker, T. R., et al. (2004), Increasing biomass in Amazonian forest plots, *Philos. Trans. R. Soc., Ser. Bs*, *359*(1443), 353–365, doi:10.1098/rstb.2003.1422.

Bousquet, P., P. Peylin, P. Ciais, C. LeQuéré, P. Friedlingstein, and P. P. Tans (2000), Regional changes in carbon dioxide fluxes of land and oceans since 1980, *Science*, *290*, 1342–1346.

Broecker, W. S., and T.-H. Peng (1982), *Tracers In The Sea*, Lamont-Doherty Earth Obs., Palisades, N. Y.

Chou, W. W., S. C. Wofsy, R. C. Harriss, J. C. Lin, C. Gerbig, and G. W. Sachse (2002), Net fluxes of CO_2 in Amazonia derived from aircraft observations, *J. Geophys. Res.*, *107*(D22), 4614, doi:10.1029/2001JD001295.

Cramer, W., D. W. Kicklighter, A. Bondeau, B. Moore, C. Churkina, B. Nemry, A. Ruimy, and A. L. Schloss (1999), Comparing global models of terrestrial net primary productivity (NPP): Overview and key results, *Global Change Biol.*, Suppl. 1, *5*, 1–15.

DeFries, R. S., R. A. Houghton, M. C. Hansen, C. B. Field, D. Skole, and J. Townshend (2002), Carbon emissions from tropical deforestation and regrowth based on satellite observations for the 1980s and 1990s, *Proc. Natl. Acad. Sci. U. S. A.*, *99*(22), 14,256–14,261.

Denning, A. S., I. Y. Fung, and D. Randall (1995), Latitudinal gradient of atmospheric CO_2 due to seasonal exchange with land biota, *Nature*, *376*(6537), 240–243.

Doney, S. C., et al. (2004), Evaluating global ocean carbon models: The importance of realistic physics, *Global Biogeochem. Cycles*, *18*, GB3017, doi:10.1029/2003GB002150.

Engelen, R. J., A. S. Denning, and K. R. Gurney (2002), On error estimation in atmospheric CO_2 inversions, *J. Geophys. Res.*, *107*(D22), 4635, doi:10.1029/2002JD002195.

Enting, I. G., and J. V. Mansbridge (1991), Latitudinal distribution of sources and sinks of CO_2—Results of an inversion study, *Tellus, Ser. B*, *43*, 156–170.

Fan, S.-M., M. Gloor, J. Mahlman, S. Pacala, J. L. Sarmiento, T. Takahashi, and P. Tans (1998), A large terrestrial carbon sink in North America implied by atmospheric and oceanic carbon dioxide data and models, *Science*, *282*, 442–446.

Fan, S.-M., J. L. Sarmiento, M. Gloor, and S. Pacala (1999), On the use of regularization techniques in the inverse modeling of atmospheric carbon dioxide, *J. Geophys. Res.*, *104*(D17), 21,503–21,512.

Feely, R. A., R. Wanninkhof, T. Takahashi, and P. Tans (1999), Influence of El Niño on the equatorial Pacific contribution to atmospheric CO_2 accumulation, *Nature*, *398*, 597–601.

Feely, R. A., C. L. Sabine, T. Takahashi, and R. Wanninkhof (2001), Uptake and storage of carbon dioxide in the ocean: The global CO_2 survey, *Oceanography*, *14*(4), 18–32.

Feely, R. A., R. Wanninkhof, W. McGillis, M. E. Carr, and C. E. Cosca (2004), Effects of wind speed and gas exchange parameterizations on the air-sea CO_2 fluxes in the equatorial Pacific Ocean, *J. Geophys. Res.*, *109*, C08S03, doi:10.1029/2003JC001896.

Food and Agriculture Organization (2001), Global forest resources assessment 2000: Main report, *For. Pap. 140*, Rome.

Fung, I., and T. Takahashi (2000), Estimating air-sea exchanges of CO_2 from pCO_2 gradients: Assessment of uncertainties, in *The Carbon Cycle*, edited by T. Wigley and D. Schimel, pp. 125–133, Cambridge Univ. Press, New York.

Gloor, M., N. Gruber, J. Sarmiento, C. L. Sabine, R. A. Feely, and C. Rödenbeck (2003), A first estimate of present and preindustrial air-sea CO_2 flux patterns based on ocean interior carbon measurements and models, *Geophys. Res. Lett.*, *30*(1), 1010, doi:10.1029/2002GL015594.

Gnanadesikan, A., and R. W. Hallberg (2000), On the relationship of the circumpolar current to Southern Hemisphere winds in coarse-resolution ocean models, *J. Phys. Oceanogr.*, *30*, 2013–2034.

Gnanadesikan, A., J. P. Dunne, R. M. Key, K. Matsumoto, J. L. Sarmiento, R. D. Slater, and P. S. Swathi (2004), Oceanic ventilation and biogeochemical cycling: Understanding the physical mechanisms that produce realistic distributions of tracers and productivity, *Global Biogeochem. Cycles*, *18*, GB4010, doi:10.1029/2003GB002097.

Gurney, K. R., et al. (2002), Towards robust regional estimates of CO_2 sources and sinks using atmospheric transport models, *Nature*, *415*, 626–630.

Gurney, K. R., et al. (2003), TransCom 3 CO_2 inversion intercomparison: 1. Annual mean control results and sensitivity to transport and prior flux information, *Tellus, Ser. B*, *55*, 555–579.

Gurney, K. R., et al. (2004), Transcom 3 inversion intercomparison: Model mean results for the estimation of seasonal carbon sources and sinks, *Global Biogeochem. Cycles*, *18*, GB1010, doi:10.1029/2003GB002111.

Heimann, M. (2001), Atmospheric inversion calculations performed for IPCC Third Assessment, *Tech. Rep. 2*, Max-Planck Inst. für Biogeochem., Jena, Germany.

Houghton, R. A. (2003a), Why are estimates of the terrestrial carbon balance so different?, *Global Change Biol.*, *9*(4), 500–509.

Houghton, R. A. (2003b), Revised estimates of the annual net flux of carbon to the atmosphere from changes in land use and land management 1850–2000, *Tellus, Ser. B*, *55*, 378–390.

Jacobson, A. R., N. Gruber, J. L. Sarmiento, M. Gloor, and S. E. Mikaloff Fletcher (2007), A joint atmosphere-ocean inversion for surface fluxes of carbon dioxide: 1. Methods and global-scale fluxes, *Global Biogeochem. Cycles*, doi:10.1029/2005GB002556, in press.

Kaminski, T., P. J. Rayner, M. Heimann, and I. G. Enting (2001), On aggregation errors in atmospheric transport inversions, *J. Geophys. Res.*, *106*(D5), 4703–4715.

Le Quéré, C., et al. (2003), Two decades of ocean CO_2 sink and variability, *Tellus, Ser. B*, *55*, 649–656.

Lucht, W., I. C. Prentice, R. B. Myneni, S. Sitch, P. Friedlingstein, W. Cramer, P. Bousquet, W. Buermann, and B. Smith (2002), Climatic control of the high-latitude vegetation greening trend and Pinatubo effect, *Science*, *296*, 1687–1689.

Malhi, Y., A. D. Nobre, J. Grace, B. Kruijt, M. G. P. Pereira, A. Culf, and S. Scott (1998), Carbon dioxide transfer over a Central Amazonian rain forest, *J. Geophys. Res.*, *103*(D24), 31,593–31,612.

Matsumoto, K., and N. Gruber (2005), How accurate is the estimation of anthropogenic carbon in the ocean? An evaluation of the ΔC^* method, *Global Biogeochem. Cycles*, *19*, GB3014, doi:10.1029/2004GB002397.

Matsumoto, K., et al. (2004), Evaluation of ocean carbon cycle models with data-based metrics, *Geophys. Res. Lett.*, *31*, L07303, doi:10.1029/2003GL018970.

McGuire, A. D., et al. (2001), Carbon balance of the terrestrial biosphere in the twentieth century: Analyses of CO_2, climate and land use effects with four process-based ecosystem models, *Global Biogeochem. Cycles*, *15*(1), 183–206.

McKinley, G. A., M. J. Follows, and J. Marshall (2003), Interannual variability of air-sea O_2 fluxes and the determination of CO_2 sinks using atmospheric O_2/N_2, *Geophys. Res. Lett.*, *30*(3), 1101, doi:10.1029/2002GL016044.

Mikaloff Fletcher, S. E., et al. (2006), Inverse estimates of anthropogenic CO_2 uptake, transport, and storage by the ocean, *Global Biogeochem. Cycles*, *20*, GB2002, doi:10.1029/2005GB002530.

Miller, S. D., M. L. Goulden, M. C. Menton, H. R. da Rocha, H. C. de Freitas, A. Figueira, and C. A. D. de Sousa (2004), Biometric and micrometeorological measurements of tropical forest carbon balance, *Ecol. Appl.*, *14*(4), Suppl. 1, S114–S126.

Murnane, R. J., J. L. Sarmiento, and C. L. Quéré (1999), Spatial distribution of air-sea CO_2 fluxes and the interhemispheric transport of carbon by the oceans, *Global Biogeochem. Cycles*, *13*(2), 287–305.

Orr, J. C., et al. (2001), Estimates of anthropogenic carbon uptake from four three-dimensional global ocean models, *Global Biogeochem. Cycles*, *15*(1), 43–60.

Phillips, O. L., et al. (2002), Increasing dominance of large lianas in Amazonian forests, *Nature*, *418*, 770–774.

Prentice, I., et al. (2001), The carbon cycle and atmospheric carbon dioxide, in *Climate Change 2001: The Scientific Basis*, edited by J. T. Houghton et al., pp. 183–237, Cambridge Univ. Press, New York.

Rödenbeck, C., S. Houweling, M. Gloor, and M. Heimann (2003a), Time-dependent atmospheric CO_2 inversions based on interannually varying tracer transport, *Tellus, Ser. B*, *55*, 488–497.

Rödenbeck, C., S. Houweling, M. Gloor, and M. Heimann (2003b), CO_2 flux history 1982–2001 inferred from atmospheric data using a global inversion of atmospheric transport, *Atmos. Chem. Phys.*, *3*, 1919–1964.

Sarmiento, J. L., N. Gruber, M. A. Brzezinski, and J. P. Dunne (2004), High-latitude controls of thermocline nutrients and low latitude biological productivity, *Nature*, *427*, 56–60.

Schimel, D. S., et al. (2001), Recent patterns and mechanisms of carbon exchange by terrestrial ecosystems, *Nature*, *414*, 169–172.

Schneider, B., R. Schlitzer, G. Fischer, and E. M. Nothig (2003), Depth-dependent elemental compositions of particulate organic matter (POM) in the ocean, *Global Biogeochem. Cycles*, *17*(2), 1032, doi:10.1029/2002GB001871.

Sigman, D. M., and E. A. Boyle (2000), Glacial/interglacial variations in atmospheric carbon dioxide, *Nature*, *407*, 859–869.

Suntharalingam, P., J. T. Randerson, N. Krakauer, D. J. Jacob, and J. A. Logan (2005), Influence of reduced carbon emissions and oxidation on the distribution of atmospheric CO_2: Implications for inversion analyses, *Global Biogeochem. Cycles*, *19*, GB4003, doi:10.1029/2005GB002466.

Takahashi, T., R. A. Feely, R. F. Weiss, D. W. Chipman, N. Bates, J. Olaffson, C. Sabine, and S. C. Sutherland (1999), Net sea-air CO_2 flux over the global oceans: An improved estimate based on the sea-air pCO_2 difference, in *2nd International Symposium, CO_2 in the Oceans*, edited by Y. Nojiri, pp. 9–14, Cent. for Global Environ. Res., Natl. Inst. for Environ. Stud., Tsukuba, Japan.

Takahashi, T., et al. (2002), Global air-sea CO_2 flux based on climatological surface ocean pCO_2, and seasonal biological and temperature effects, *Deep Sea Res., Part II*, *49*, 1601–1622.

Tans, P. P., I. Y. Fung, and T. Takahashi (1990), Observational constraints on the global atmospheric CO_2 budget, *Science*, *247*, 1431–1438.

Wanninkhof, R., and W. R. McGillis (1999), A cubic relationship between air-sea CO_2 exchange and wind speed, *Geophys. Res. Lett.*, *26*(13), 1889–1892.

M. Gloor, A. R. Jacobson, and J. L. Sarmiento, Atmospheric and Oceanic Sciences Program, Princeton University, P.O. Box CN710, Princeton, NJ 08544-0710, USA. (andy.jacobson@noaa.gov)

N. Gruber and S. E. Mikaloff Fletcher, Department of Atmospheric and Oceanic Sciences, University of California, Los Angeles, CA 90032, USA.